PNAS
www.pnas.org

Supplementary Information for

Thinner biological tissues induce leaflet flutter in aortic heart valve replacements

Emily L. Johnson, Michael C. H. Wu, Fei Xu, Nelson M. Wiese, Manoj R. Rajanna, Austin J. Herrema, Baskar Ganapathysubramanian, Thomas J. R. Hughes, Michael S. Sacks, and Ming-Chen Hsu

Corresponding Authors:
Thomas J. R. Hughes (E-mail: hughes@oden.utexas.edu)
Michael S. Sacks (E-mail: msacks@oden.utexas.edu)
Ming-Chen Hsu (E-mail: jmchsu@iastate.edu)

This PDF file includes:

Other supplementary materials for this manuscript include the following:

Supplementary Tables

Table S1. Quantified results of the filtered flutter signals shown in Fig. 7. $E_{LC}^{leaflet}$ indicates the signal energy on the left coronary leaflet. H_1 and V_2 indicate the free edge and the central vertical leaflet tracking curve on the valve, respectively, as shown in Fig. 1*C*. The locations of the peak frequency and wavenumber are denoted as f_{LC}^{peak} and ξ_{LC}^{peak}, respectively, and the peak amplitude is denoted as A_{LC}^{peak}.

	BP-100	BP-75	BP-50	BP-25
H_1 $E_{LC}^{leaflet}$ (cm^2)	3.27×10^0	4.73×10^0	3.68×10^2	5.80×10^1
H_1 f_{LC}^{peak} (Hz)	20.0	20.0	50.0	55.0
H_1 ξ_{LC}^{peak} (cm^{-1})	0.0	0.0	0.0	0.0
H_1 A_{LC}^{peak} (cm)	0.0053	0.0064	0.0510	0.0132
V_2 $E_{LC}^{leaflet}$ (cm^2)	1.02×10^1	2.33×10^0	3.02×10^2	2.12×10^1
V_2 f_{LC}^{peak} (Hz)	20.0	20.0	50.0	20.0
V_2 ξ_{LC}^{peak} (cm^{-1})	0.0	0.0	0.0	0.0
V_2 A_{LC}^{peak} (cm)	0.0080	0.0051	0.0422	0.0090

Table S2. Quantified results from leaflet tracking curve H_1 of the filtered flutter signal energy on each valve leaflet for each cardiac cycle. $E_{LC}^{leaflet}$, $E_{RC}^{leaflet}$, and $E_{NC}^{leaflet}$ indicate the signal energy on the left coronary, right coronary, and non-coronary leaflets, respectively. The three individual cardiac cycles are denoted as $Cycle_A$, $Cycle_B$, and $Cycle_C$.

	BP-100	BP-75	BP-50	BP-25
$Cycle_A$ $E_{LC}^{leaflet}$	3.27×10^0	4.73×10^0	3.68×10^2	5.80×10^1
$Cycle_B$ $E_{LC}^{leaflet}$	3.35×10^0	5.11×10^0	2.42×10^2	6.21×10^1
$Cycle_C$ $E_{LC}^{leaflet}$	3.45×10^0	5.91×10^0	3.24×10^2	5.31×10^1
$Cycle_A$ $E_{RC}^{leaflet}$	2.65×10^0	5.57×10^0	3.03×10^2	1.13×10^2
$Cycle_B$ $E_{RC}^{leaflet}$	4.23×10^0	5.38×10^0	2.09×10^2	5.05×10^1
$Cycle_C$ $E_{RC}^{leaflet}$	3.25×10^0	4.37×10^0	2.27×10^2	3.50×10^1
$Cycle_A$ $E_{NC}^{leaflet}$	2.27×10^0	3.21×10^0	2.12×10^2	7.00×10^1
$Cycle_B$ $E_{NC}^{leaflet}$	2.92×10^0	2.89×10^0	1.81×10^2	5.72×10^1
$Cycle_C$ $E_{NC}^{leaflet}$	3.12×10^0	2.82×10^0	2.53×10^2	4.86×10^1

Table S3. Quantified results from leaflet tracking curve V_2 of the filtered flutter signal energy on each valve leaflet for each cardiac cycle. $E_{LC}^{leaflet}$, $E_{RC}^{leaflet}$, and $E_{NC}^{leaflet}$ indicate the signal energy on the left coronary, right coronary, and non-coronary leaflets, respectively. The three individual cardiac cycles are denoted as $Cycle_A$, $Cycle_B$, and $Cycle_C$.

	BP-100	BP-75	BP-50	BP-25
$Cycle_A$ $E_{LC}^{leaflet}$	1.02×10^1	2.33×10^0	3.02×10^2	2.12×10^1
$Cycle_B$ $E_{LC}^{leaflet}$	1.04×10^1	2.01×10^0	2.41×10^2	2.34×10^1
$Cycle_C$ $E_{LC}^{leaflet}$	1.13×10^1	2.50×10^0	2.88×10^2	2.18×10^1
$Cycle_A$ $E_{RC}^{leaflet}$	9.64×10^0	2.45×10^0	2.58×10^2	5.88×10^1
$Cycle_B$ $E_{RC}^{leaflet}$	7.99×10^0	2.22×10^0	1.88×10^2	2.10×10^1
$Cycle_C$ $E_{RC}^{leaflet}$	1.08×10^1	2.31×10^0	2.06×10^2	2.23×10^1
$Cycle_A$ $E_{NC}^{leaflet}$	1.01×10^1	2.23×10^0	2.42×10^2	4.08×10^1
$Cycle_B$ $E_{NC}^{leaflet}$	1.09×10^1	1.88×10^0	1.79×10^2	3.12×10^1
$Cycle_C$ $E_{NC}^{leaflet}$	1.04×10^1	1.92×10^0	2.70×10^2	2.75×10^1

Table S4. Quantified results of the filtered flutter signal energy averaged on the three valve leaflets over three cardiac cycles ($E_{\text{avg}}^{\text{leaflet}}$).

	BP-100	BP-75	BP-50	BP-25
H_1 $E_{\text{avg}}^{\text{leaflet}}$	3.17×10^{0}	4.44×10^{0}	2.57×10^{2}	6.09×10^{1}
H_2 $E_{\text{avg}}^{\text{leaflet}}$	2.10×10^{0}	1.79×10^{0}	1.09×10^{2}	2.63×10^{1}
H_3 $E_{\text{avg}}^{\text{leaflet}}$	2.69×10^{0}	6.69×10^{-1}	4.67×10^{1}	1.28×10^{1}
H_4 $E_{\text{avg}}^{\text{leaflet}}$	1.20×10^{1}	1.31×10^{0}	1.69×10^{1}	8.25×10^{0}
V_1 $E_{\text{avg}}^{\text{leaflet}}$	3.42×10^{0}	1.56×10^{0}	3.33×10^{1}	1.70×10^{1}
V_2 $E_{\text{avg}}^{\text{leaflet}}$	1.02×10^{1}	2.20×10^{0}	2.42×10^{2}	2.98×10^{1}
V_3 $E_{\text{avg}}^{\text{leaflet}}$	3.48×10^{0}	1.53×10^{0}	3.04×10^{1}	2.51×10^{1}

Table S5. Energy efficiency of each valve. The energy efficiency is defined as the ratio between flow energy exiting and entering the aorta during one cardiac cycle. η denotes the energy efficiency and ϵ denotes the relative difference with respect to the BP-100 case.

	BP-100	BP-75	BP-50	BP-25
η (%)	91.16	91.70	90.69	91.31
ϵ (%)	0.00	0.60	−0.51	0.16

Supplementary Figures

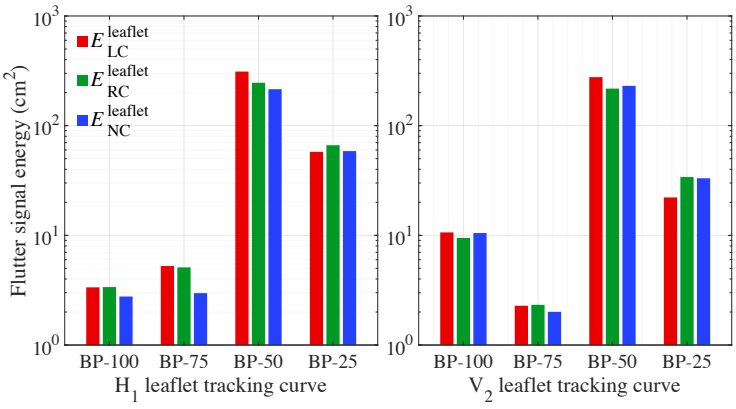

Fig. S1. Quantified results of the flutter signal energy on each leaflet averaged over three cardiac cycles for tracking curves H_1 (*Left*) and V_2 (*Right*). $E^{\text{leaflet}}_{\text{LC}}$, $E^{\text{leaflet}}_{\text{RC}}$, and $E^{\text{leaflet}}_{\text{NC}}$ indicate the signal energy on the left coronary, right coronary, and non-coronary leaflets, respectively, averaged over three cardiac cycles. H_1 and V_2 indicate the free edge and the central vertical leaflet tracking curve on the valve, respectively, as shown in Fig. 1*C*.

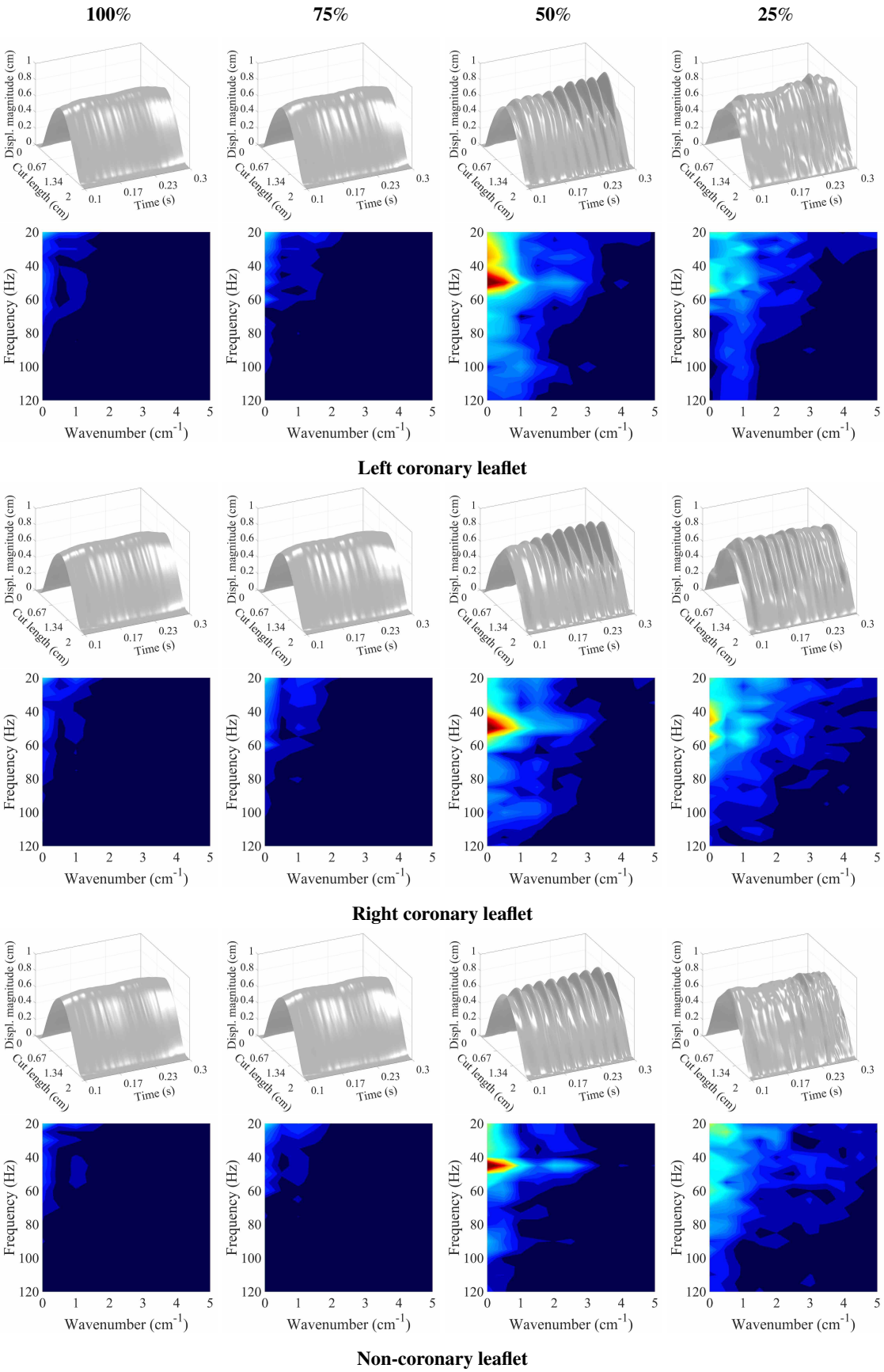

Fig. S2. Horizontal leaflet tracking curve one (H_1). Displacement magnitude visualization of the leaflet tracking curves throughout the t = 0.1- to 0.3-s period of $Cycle_A$. Cut length denotes the length of each tracking curve. 2D top view of the frequency domain visualization from the discrete Fourier transform operations on the displacement magnitude data.

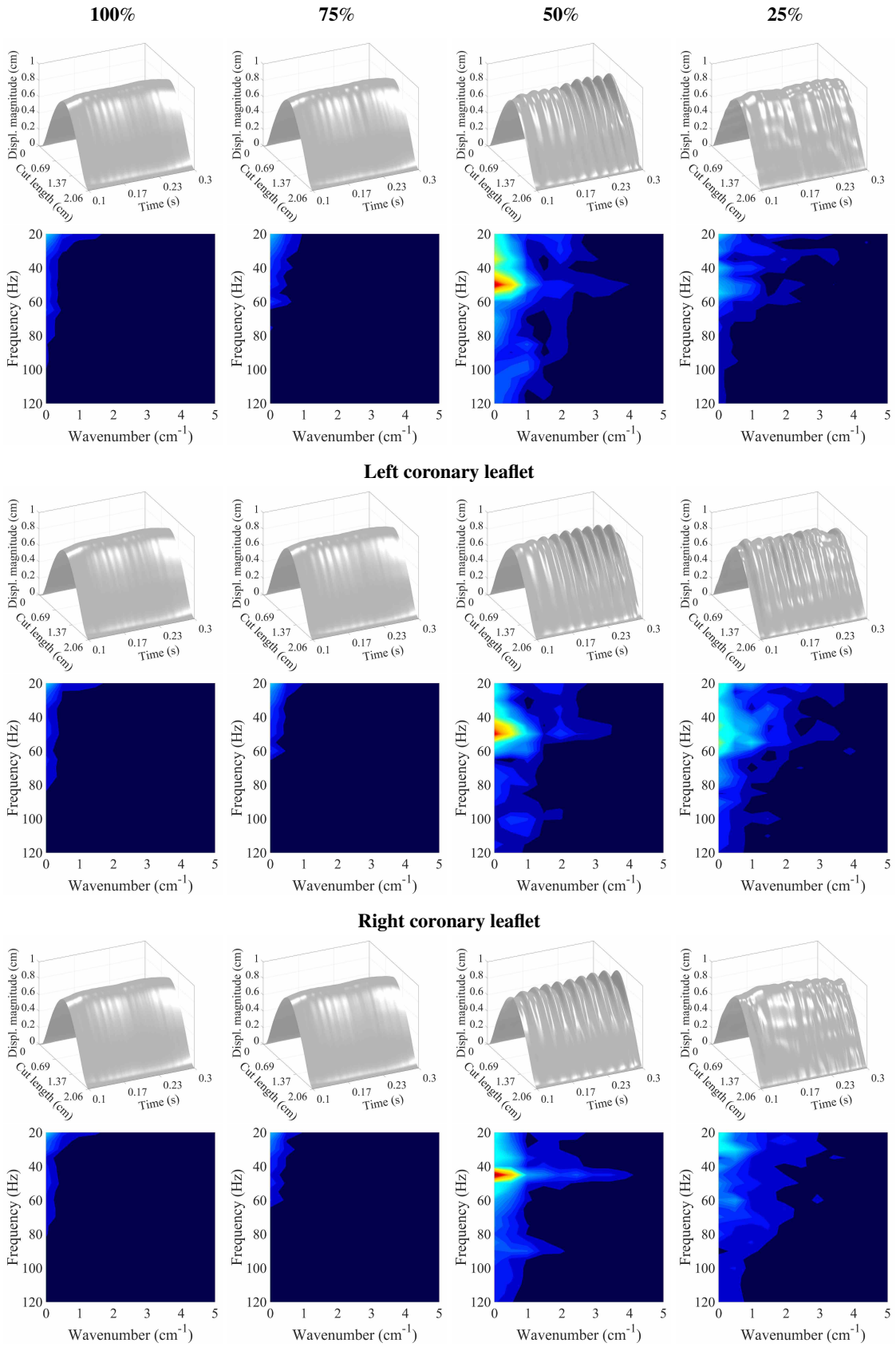

Fig. S3. Horizontal leaflet tracking curve two (H_2). Displacement magnitude visualization of the leaflet tracking curves throughout the t = 0.1- to 0.3-s period of Cycle$_A$. Cut length denotes the length of each tracking curve. 2D top view of the frequency domain visualization from the discrete Fourier transform operations on the displacement magnitude data.

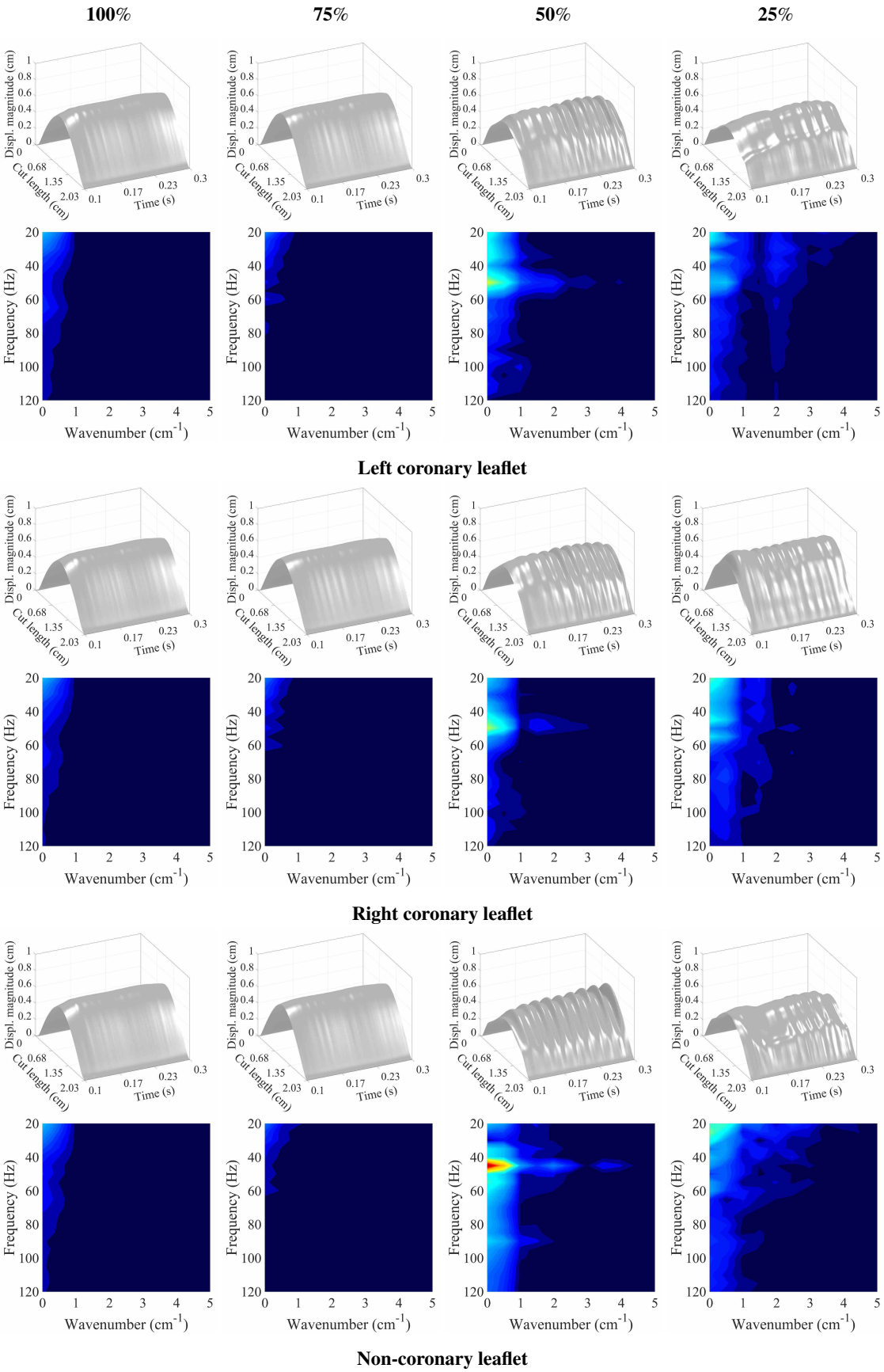

Fig. S4. Horizontal leaflet tracking curve three (H_3). Displacement magnitude visualization of the leaflet tracking curves throughout the t = 0.1- to 0.3-s period of $Cycle_A$. Cut length denotes the length of each tracking curve. 2D top view of the frequency domain visualization from the discrete Fourier transform operations on the displacement magnitude data.

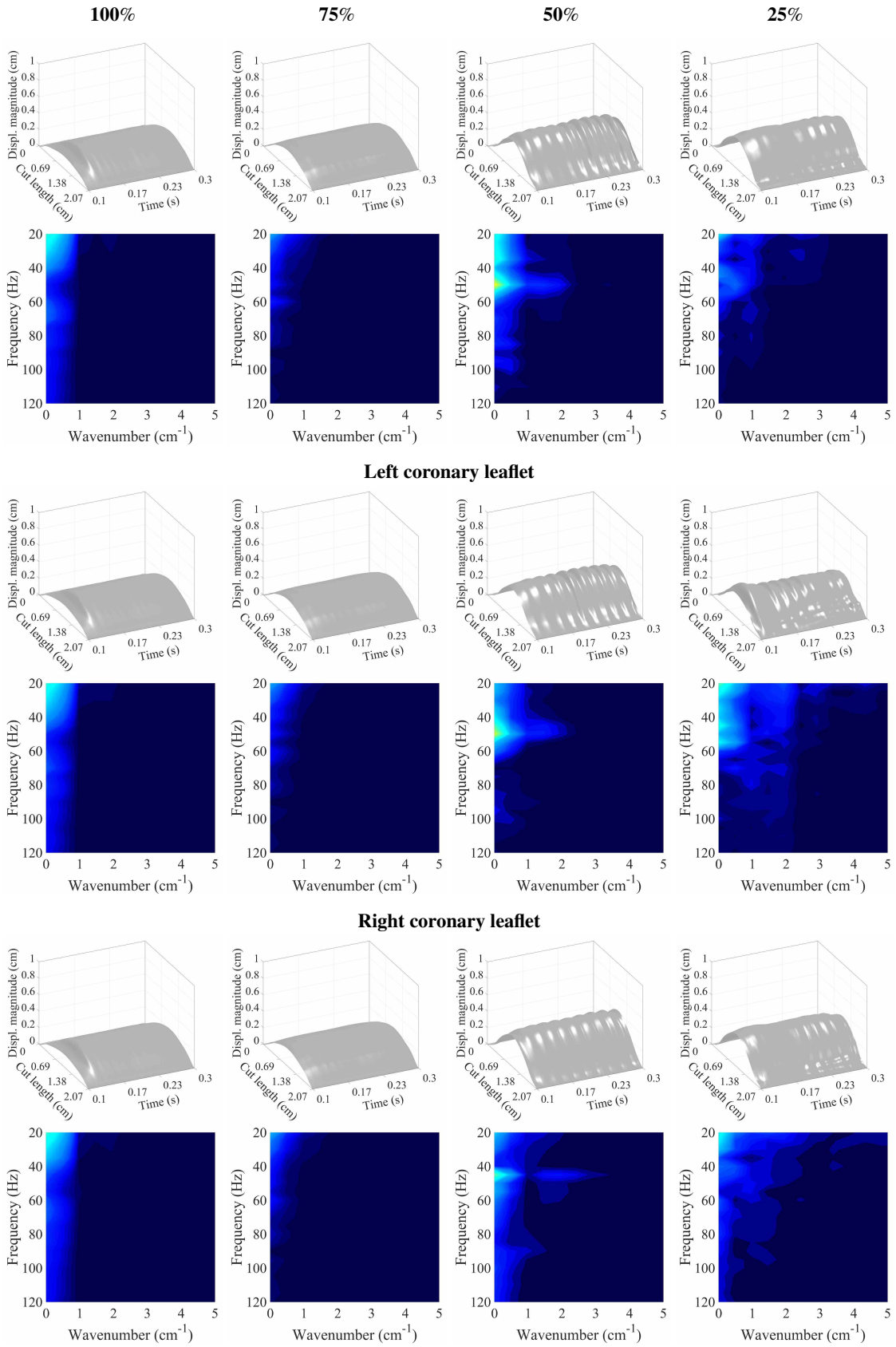

Fig. S5. Horizontal leaflet tracking curve four (H_4). Displacement magnitude visualization of the leaflet tracking curves throughout the t = 0.1- to 0.3-s period of $Cycle_A$. Cut length denotes the length of each tracking curve. 2D top view of the frequency domain visualization from the discrete Fourier transform operations on the displacement magnitude data.

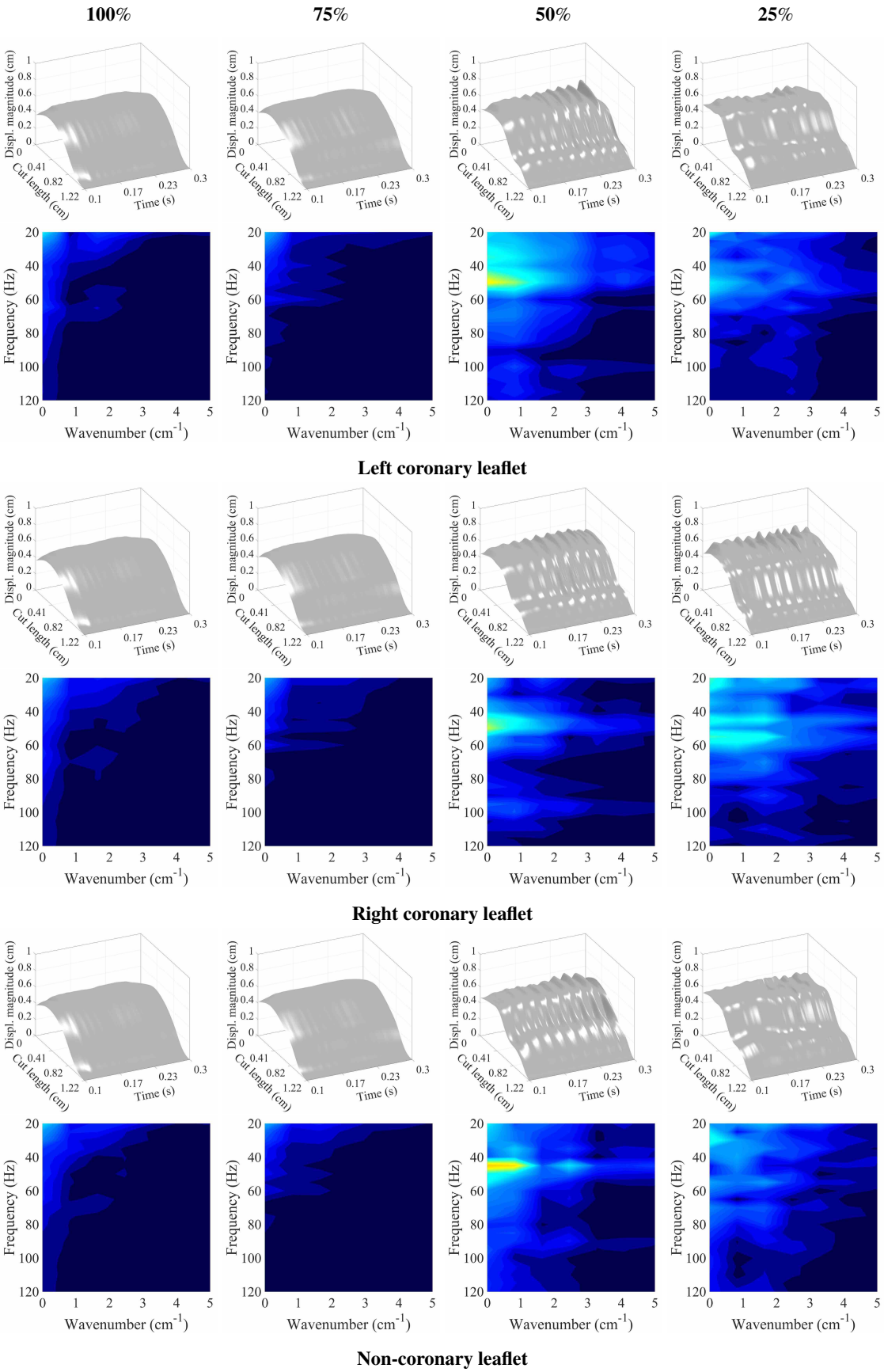

Fig. S6. Vertical leaflet tracking curve one (V_1). Displacement magnitude visualization of the leaflet tracking curves throughout the t = 0.1- to 0.3-s period of Cycle_A. Cut length denotes the length of each tracking curve. 2D top view of the frequency domain visualization from the discrete Fourier transform operations on the displacement magnitude data.

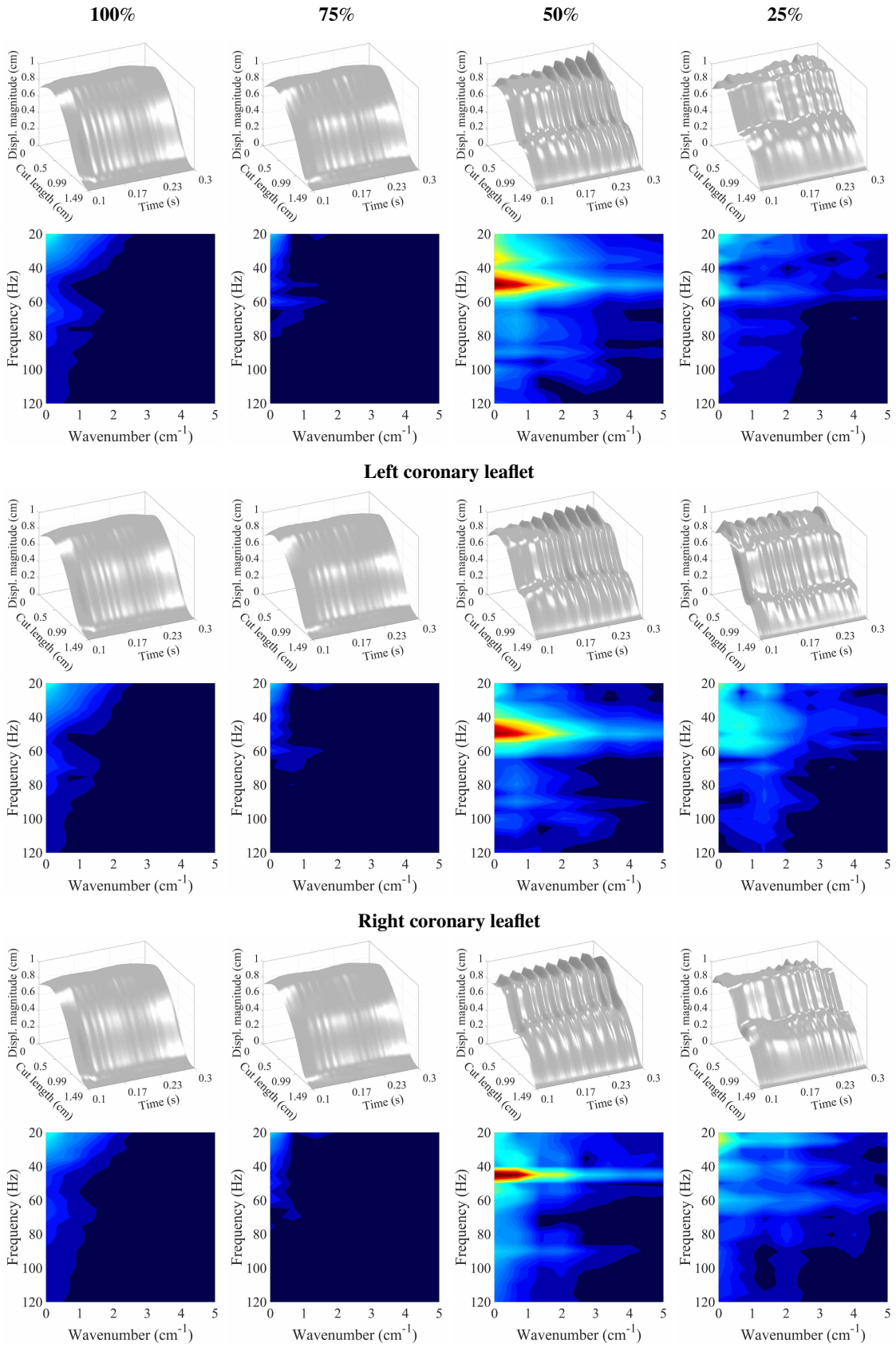

Fig. S7. Vertical leaflet tracking curve two (V_2). Displacement magnitude visualization of the leaflet tracking curves throughout the t = 0.1- to 0.3-s period of $Cycle_A$. Cut length denotes the length of each tracking curve. 2D top view of the frequency domain visualization from the discrete Fourier transform operations on the displacement magnitude data.

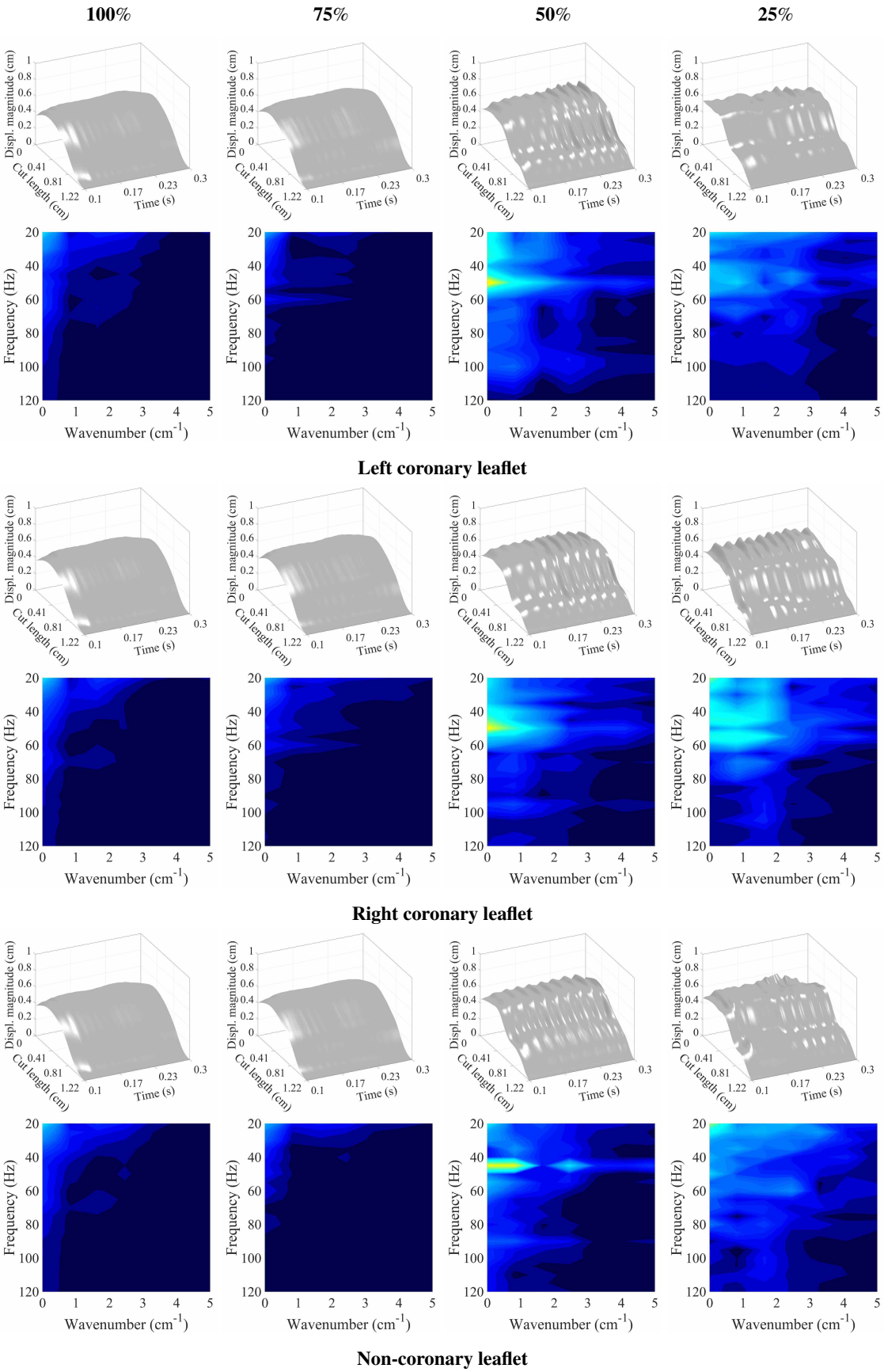

Fig. S8. Vertical leaflet tracking curve three (V_3). Displacement magnitude visualization of the leaflet tracking curves throughout the t = 0.1- to 0.3-s period of Cycle$_A$. Cut length denotes the length of each tracking curve. 2D top view of the frequency domain visualization from the discrete Fourier transform operations on the displacement magnitude data.

Supplementary Movies

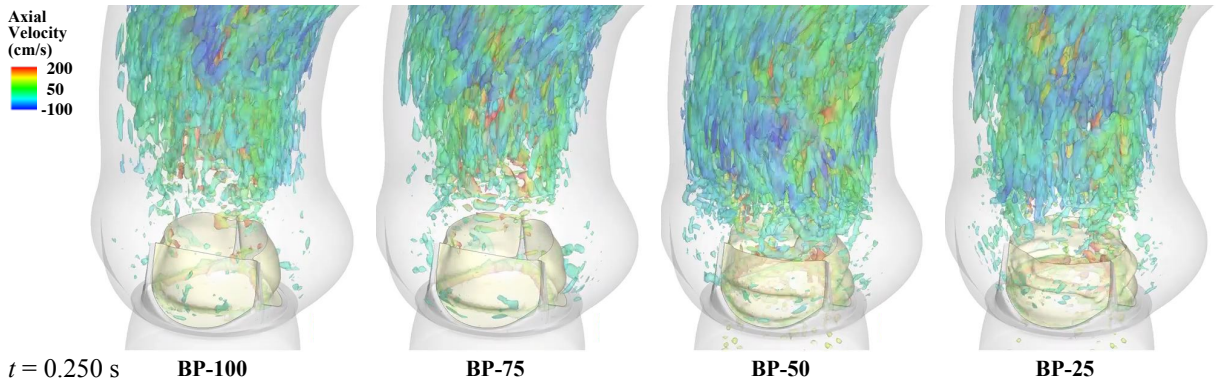

Movie S1. Vorticity isosurfaces, colored by the axial velocity, over a complete cardiac cycle for each valve thickness case.

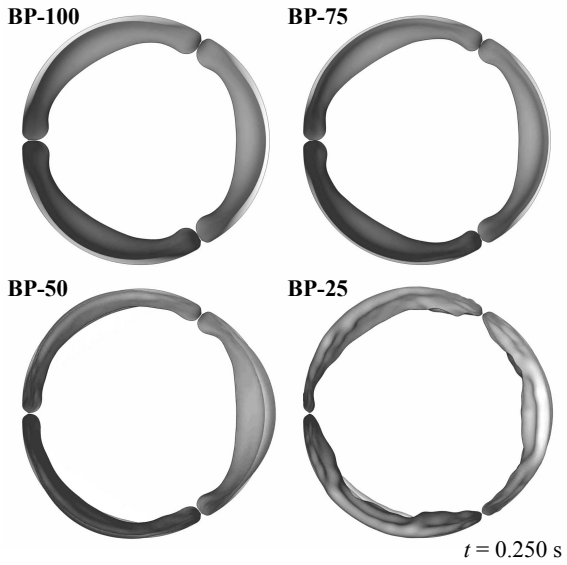

Movie S2. Top view of the valve for each thickness case for t = 0.0 to 0.4 s.

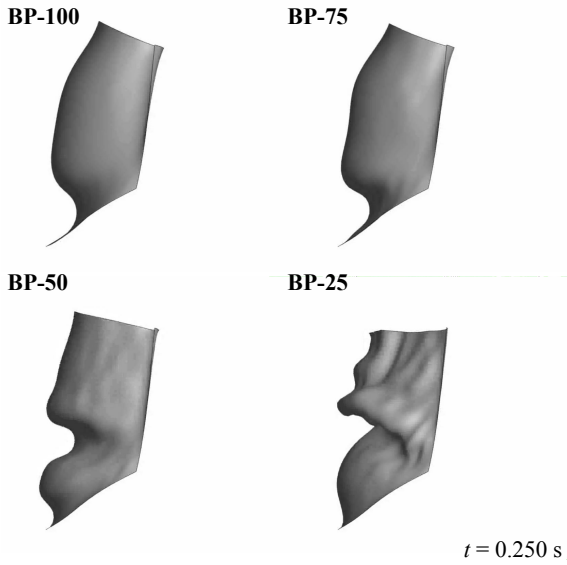

Movie S3. Side view of the valve for each thickness case for t = 0.0 to 0.4 s.

Supporting Information Text

Validation Study. Raghav et al. (1) performed an *in vitro* study on the Carpentier-Edwards PERIMOUNT Magna Ease valve using a pulsatile flow loop and reported the performance of these bioprosthetic implants within an idealized aortic geometry and left heart simulator system. The experiments were conducted at normal human physiological conditions, including specific pressure inputs and outputs that correspond to the ventricular and aortic pressures, respectively, which are shown in Fig. S9. Here, we carry out a validation study to investigate the effectiveness of our immersogeometric fluid–structure interaction (FSI) framework for bioprosthetic heart valve (BHV) simulations. We construct a volumetric nonuniform rational B-spline-based rigid aorta geometry that closely approximates the one used in the experiment and apply the pressure boundary conditions at the inlet and outlet locations using the experimental ventricular and aortic pressure profiles (Fig. S9), respectively. The other surfaces of the aorta are set as no-slip boundaries, and the fluid properties are set to match the water-glycerin solution from the experimental setup. The geometry of the BHV is modeled based on the 23 mm Magna Ease valve, and the thickness of the leaflets is set to 0.0386 cm. All other parameters for this setup are the same as those reported in *Materials and Methods*. The computational results compared to the experimental data are presented in Figs. S10 and S11. The experimental data are extracted from available video frames published by Raghav et al. (1), and the corresponding BHV simulation data is computed from the FSI results throughout the cardiac cycle. Figs. S10 *A* and *B* show the maximum open valve shapes of the experimental and computational results, respectively. For a direct comparison, these results are superimposed in Fig. S10*C* to show the qualitative resemblance between the computed leaflet deformations and the experimental images. To further validate the BHV FSI, the geometric orifice area (GOA) over a cardiac cycle is computed from the available video frames and the simulation results. The GOA results are normalized by the maximum open area of each respective valve to eliminate the effect of sizing differences in the comparison. As shown in Fig. S11, the simulation closely captures the normalized GOA behavior from the experiment, which further indicates that the FSI modeling assumptions are appropriate for predicting the dynamic behavior of heart valve leaflets immersed in physiological flow fields.

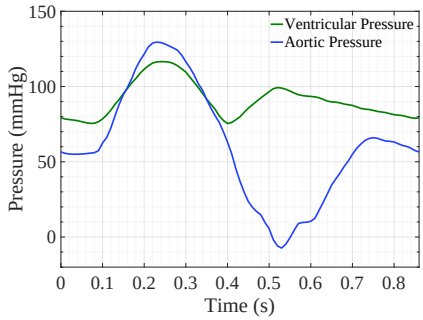

Fig. S9. Ventricular and aortic pressure profiles for the experimental and computational studies.

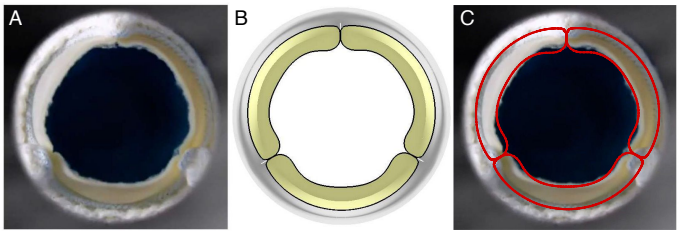

Fig. S10. Leaflet shape comparison between the experimental and computational results. The experimental results from the Magna Ease valve are obtained from Raghav et al. (1). (*A*) Maximum orifice area frame of the Magna Ease valve. (*B*) Maximum orifice area frame of the simulated BHV. (*C*) Superimposed solutions for the experimental and computational BHV results at the maximum orifice area frames. Outlines indicate the edges of the simulated valve model.

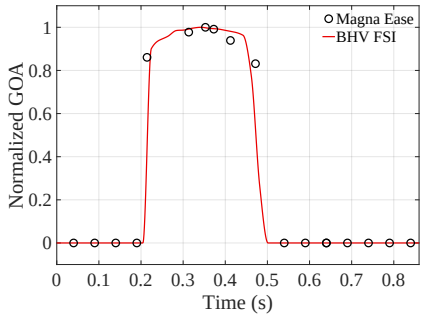

Fig. S11. Normalized orifice area data from the experimental (Magna Ease) and computational BHV results.

Pressure Waveform Study. The following pressure study examines an idealized pressure waveform to determine whether the flutter is induced by the higher frequency oscillation in the experimental pressure waveform. The BP-50 case is simulated using the idealized pressure waveform shown in Fig. S12*A*. The idealized pressure input has the same minimum and maximum values as the original experimental pressure waveform and exhibits similar low-frequency components (Fig. S12*B*). Fig. S13 shows the results for the flow quantities (Fig. S13 *A* and *B*) and valve orifice (Fig. S13*C*). These results are qualitatively and quantitatively similar to the BP-50 case under the experimental conditions, which indicates that the flutter behavior is not induced by the oscillations in the t = 0.0- to 0.3-s range of the experimental pressure waveform.

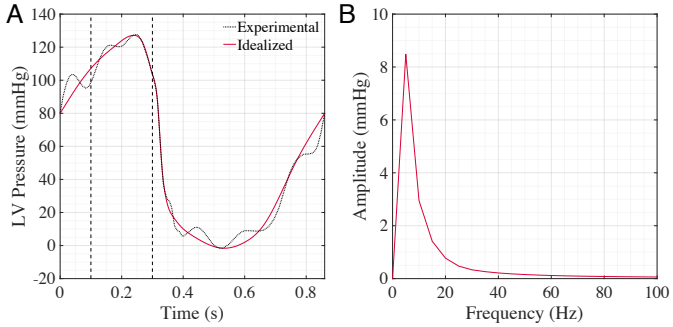

Fig. S12. Idealized approximation of the physiologically realistic left-ventricular pressure waveform from Yap et al. (2) that is applied at the inlet. (*A*) Idealized and experimental left-ventricular pressures. (*B*) Frequency domain from the discrete Fourier transform operations for t = 0.1 to 0.3 s of the idealized pressure.

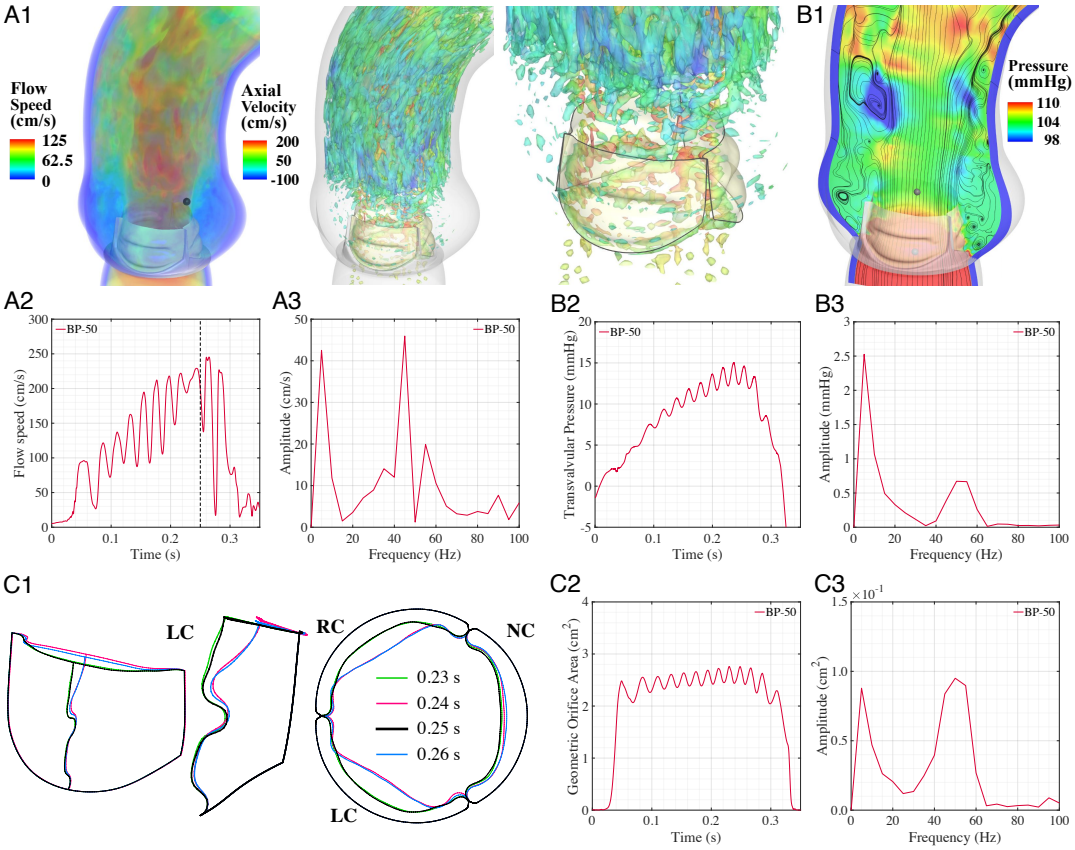

Fig. S13. Computational results from the BP-50 case simulated with an idealized inlet pressure condition. (*A1–A3*) Flow speed quantities. (*B1–B3*) Pressure field and transvalvular pressure gradient. (*C1–C3*) Leaflet shapes and geometric orifice area. *A1* shows the volume rendering visualization of the velocity field, colored by the flow speed, and vorticity isosurfaces, colored by the axial (normal to the aortic annulus) velocity, at peak opening (t = 0.25 s). The flow speed is evaluated for each valve at the indicated point. *B1* shows the pressure contours superimposed with streamlines at peak opening. The transvalvular pressure gradient is evaluated for each case as the difference between the left-ventricular pressure (0.1 cm below the annulus) and the aortic pressure (1.3 cm above the annulus) at the indicated points on each side of the valve. *C1* shows side and top views of the shape at the free edge (H_1) and at the central vertical tracking curve (V_2). The top view shows the orientation of the right coronary leaflet (RC) and non-coronary leaflet (NC) relative to the left coronary leaflet. *A2*, *B2*, and *C2* show the corresponding temporal behavior of each quantity of interest. *A3*, *B3*, and *C3* show the frequency domain from the discrete Fourier transform operations for t = 0.1 to 0.3 s of each quantity of interest.

References

1. V. Raghav *et al*., Long-term durability of carpentier-edwards magna ease valve: a one billion cycle in vitro study. *Ann. Thorac. Surg.* **101**, 1759–1765 (2016).
2. C. H. Yap, N. Saikrishnan, G. Tamilselvan, A. P. Yoganathan, Experimental technique of measuring dynamic fluid shear stress on the aortic surface of the aortic valve leaflet. *J. Biomech. Eng.* **133**, 061007 (2011).

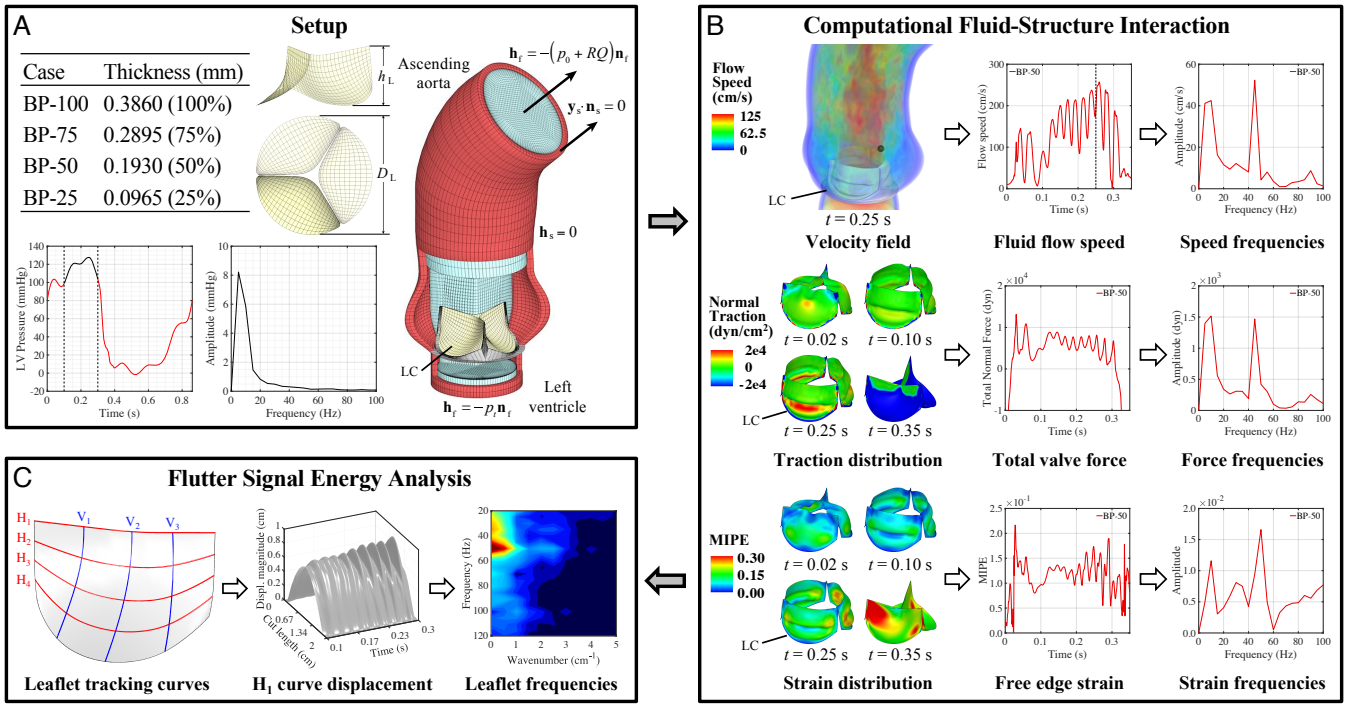

Fig. 1. Overall schematic of the FSI simulation and flutter quantification methodologies. All results and analyses show the BP-50 case. The left coronary leaflet (LC) is indicated on each geometry. Further details can be found in *Materials and Methods*. (*A*) Valve thicknesses, ventricular pressure waveform, and problem setup for the computational simulation of the aorta and valve geometry. (*B*) FSI results and signal analysis procedure for the velocity field, leaflet normal tractions, and leaflet strains. The time signals of each quantity are analyzed using discrete Fourier transform operations. (*C*) Flutter analysis methodology for the leaflet displacement. The tracking curves on the leaflet indicate the horizontal and vertical locations along which the flutter behavior is quantified.

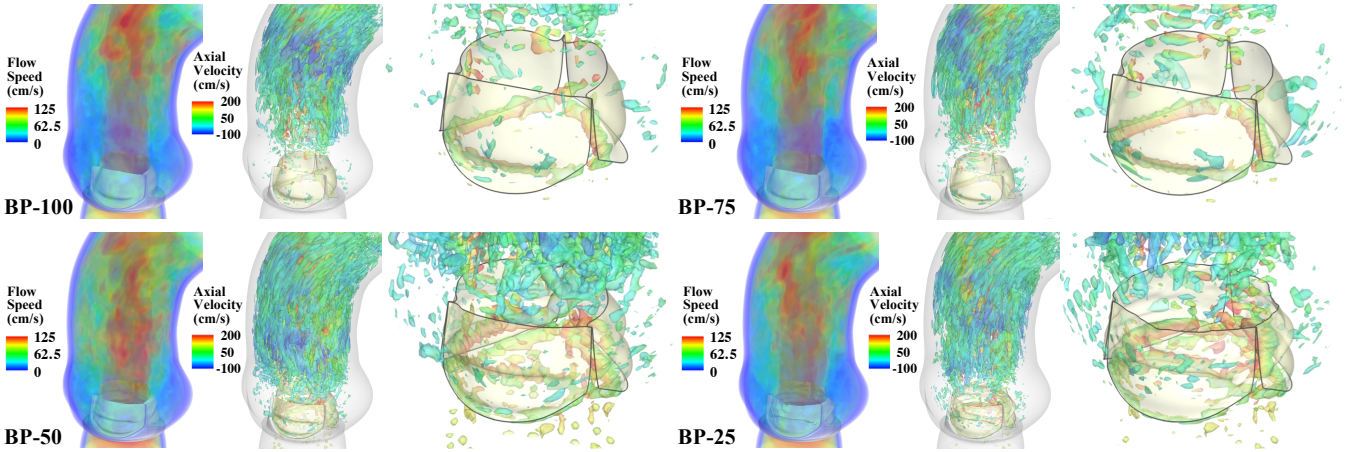

Fig. 2. FSI simulation results for each valve thickness case. Volume rendering visualization of the velocity field, colored by the flow speed, and vorticity isosurfaces, colored by the axial (normal to the aortic annulus) velocity, at peak opening (t = 0.25 s) are shown for each case.

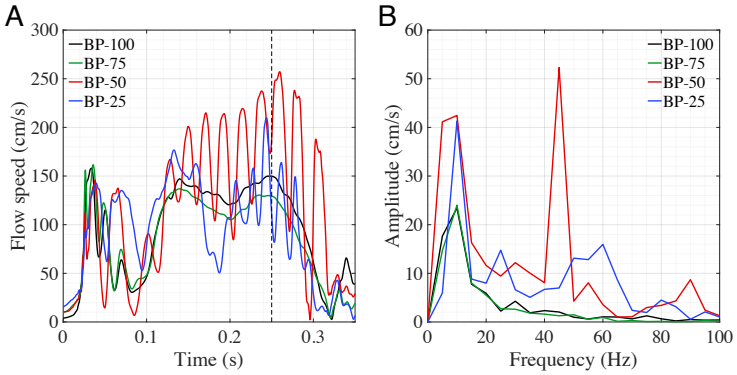

Fig. 3. Flow speed results for each valve thickness case. (*A*) The speed is evaluated for each valve at the point indicated in Fig. 1*B*. (*B*) Frequency domain from the discrete Fourier transform operations for t = 0.1 to 0.3 s of the flow speed.

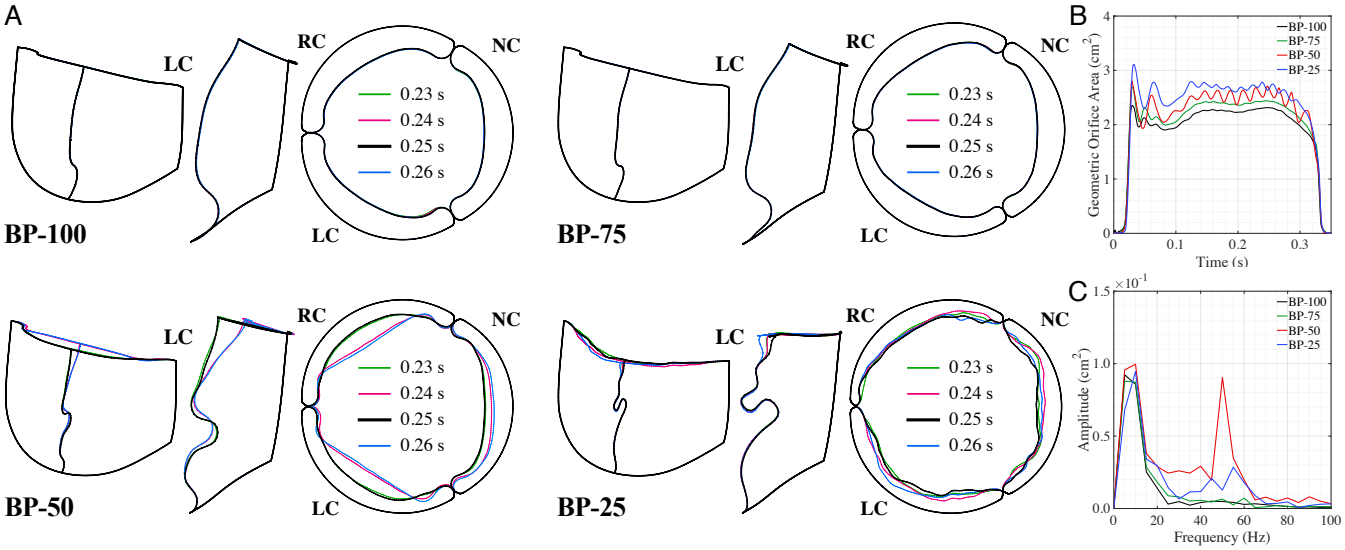

Fig. 4. Leaflet shapes at selected time instances for each valve thickness case. (*A*) Side and top views of the shape at the free edge (H_1) and at the central vertical tracking curve (V_2). The top view shows the orientation of the right coronary leaflet (RC) and non-coronary leaflet (NC) relative to the left coronary leaflet. (*B*) Projected geometric orifice area computed for each valve. (*C*) Frequency domain from the discrete Fourier transform operations for t = 0.1 to 0.3 s of the geometric orifice area.

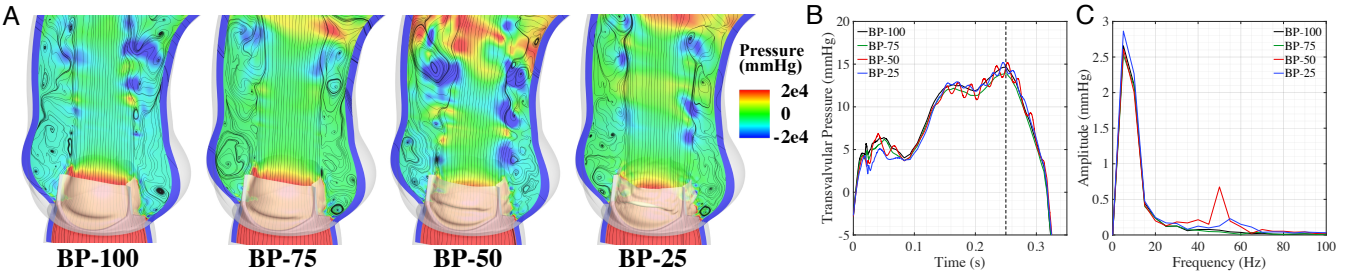

Fig. 5. Pressure field and transvalvular pressure gradient. (*A*) Pressure contours superimposed with streamlines at peak opening (t = 0.25 s). The transvalvular pressure gradient is evaluated for each case as the difference between the left ventricular pressure (0.1 cm below the annulus) and the aortic pressure (1.3 cm above the annulus) at the indicated points on each side of the valve. (*B*) Transvalvular pressure gradient across each valve. (*C*) Frequency domain from the discrete Fourier transform operations for t = 0.1 to 0.3 s of the transvalvular pressure.

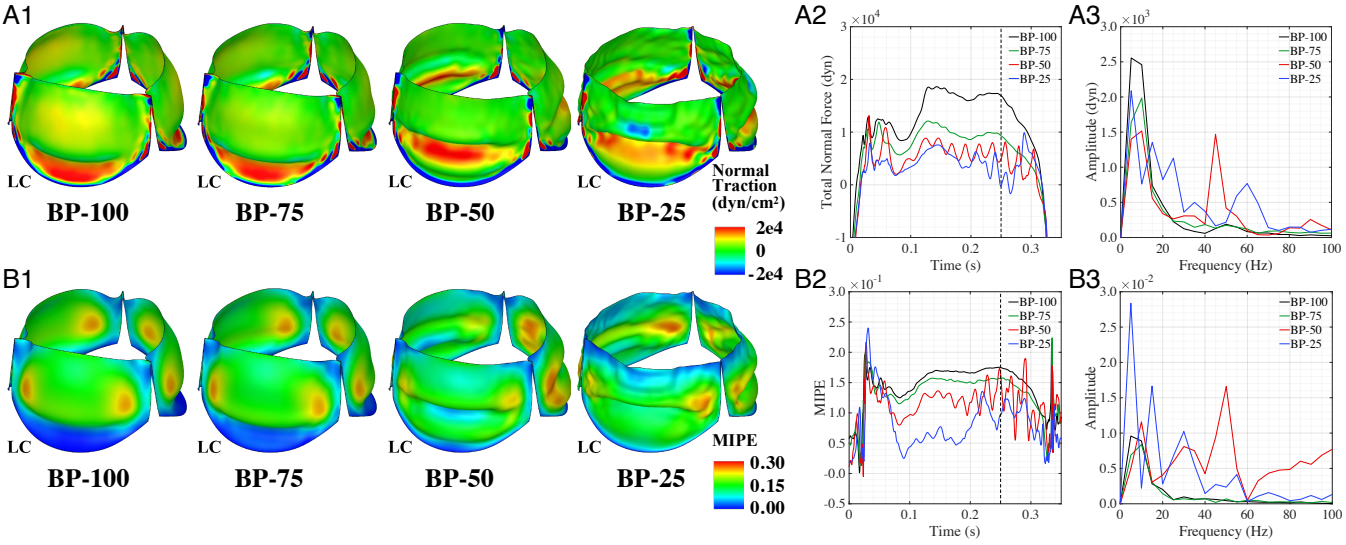

Fig. 6. Frequency analysis of force and strain information on the leaflets. (*A1*) Leaflet normal traction at peak opening (t = 0.25 s). (*A2*) Integrated normal traction on the left coronary leaflet (LC). (*A3*) Frequency domain from the discrete Fourier transform operations for t = 0.1 to 0.3 s of the integrated traction force. (*B1*) Leaflet maximum in-plane principal Green–Lagrange strain (MIPE) at peak opening (t = 0.25 s) evaluated on the aortic side of the leaflets. (*B2*) MIPE at the center of the free edge on the left coronary leaflet. (*B3*) Frequency domain from the discrete Fourier transform operations for t = 0.1 to 0.3 s of the MIPE.

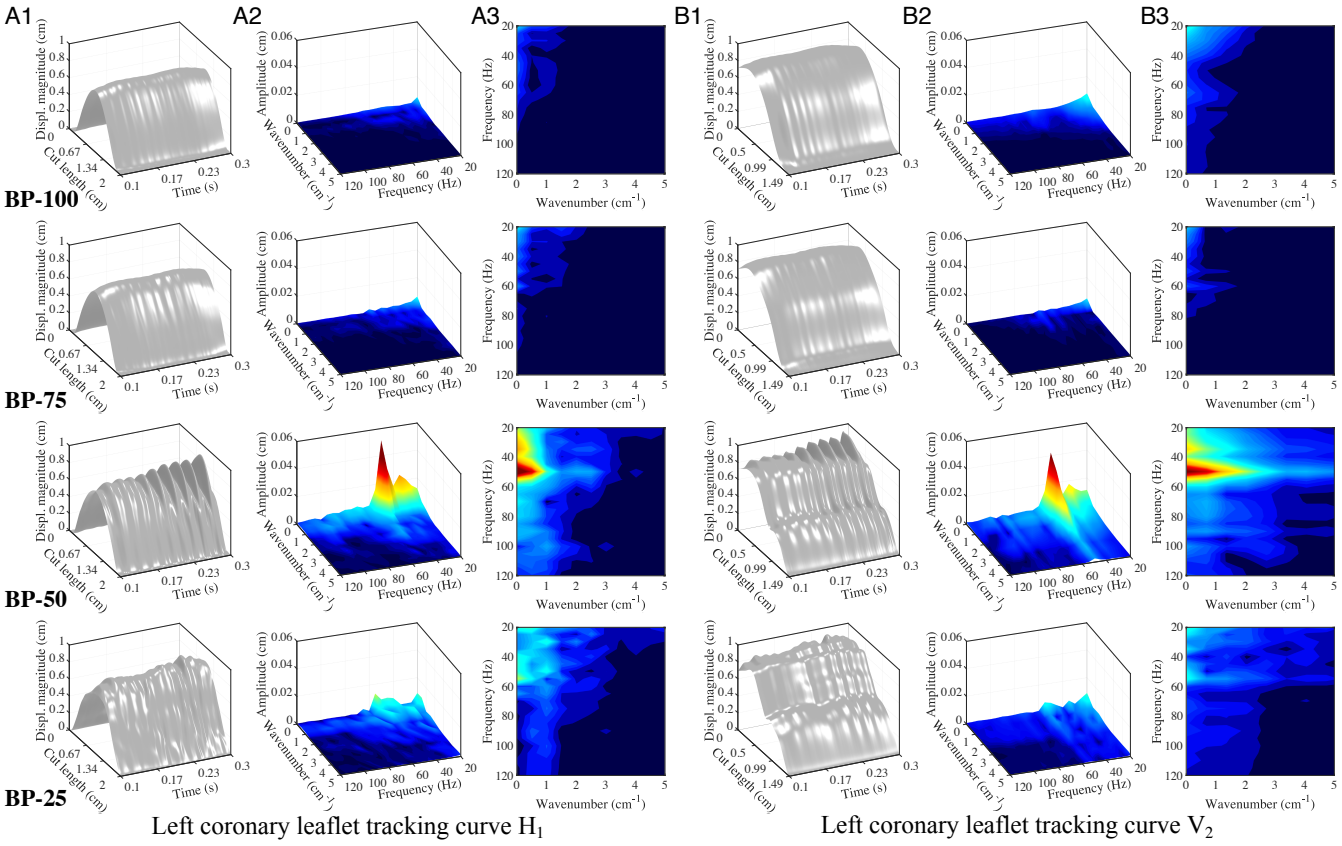

Fig. 7. Frequency analysis of the leaflet displacement. Data are tracked on horizontal tracking curve H_1 (*A1–A3*) and vertical tracking curve V_2 (*B1–B3*) on the left coronary leaflet, as shown in Fig. 1*C*. *A1* and *B1* show the displacement magnitude visualization of the leaflet tracking curves throughout the *t* 0.1- to 0.3-s portion of the valve-opening period. Cut length denotes the length of each tracking curve. *A2–A3* and *B2–B3* show the 3D view and 2D top view of the frequency domain visualization from the discrete Fourier transform operations for t = 0.1 to 0.3 s of the displacement magnitude data, respectively. The data below 20 Hz are excluded for the computation of the flutter signal energy.

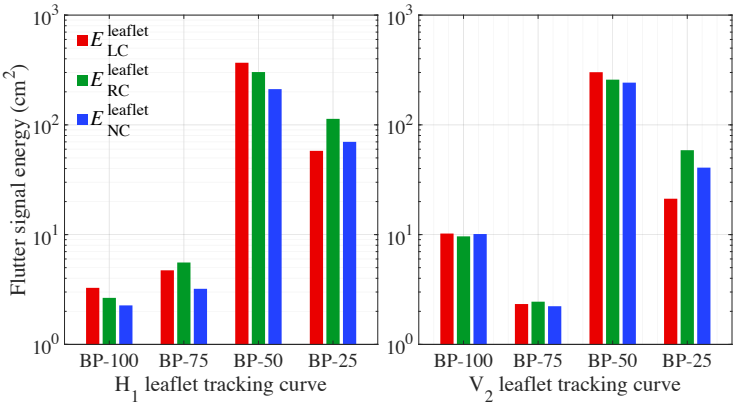

Fig. 8. Quantified results of the filtered flutter signal energy for tracking curves H_1 (*Left*) and V_2 (*Right*). $E^{\text{leaflet}}_{\text{LC}}$ indicates the signal energy on the left coronary leaflet for a single cardiac cycle. $E^{\text{leaflet}}_{\text{RC}}$ and $E^{\text{leaflet}}_{\text{NC}}$ indicate the signal energy on the right coronary and non-coronary leaflets, respectively. H_1 and V_2 indicate the free edge and the central vertical tracking curve on the leaflets, respectively, as shown in Fig. 1*C*.